Taylor & Francis
Taylor & Francis Group

Future Science OA

ISSN: 2056-5623 (Online) Journal homepage: www.tandfonline.com/journals/ifso20

Preclinical assessment of GNE^{wt}/bi-shRNA-GNE^{M743T} lipoplex product development for GNE myopathy

Fabienne Kerneis, Christopher M Jay, Donald Rao, Jeremy Winchester, Alexander Nemunaitis, Emily Nemunaitis, Ernest Bognar, Gladice Wallraven, Laura Stanbery, Adam Walter, Sep Sarshar & John Nemunaitis

To cite this article: Fabienne Kerneis, Christopher M Jay, Donald Rao, Jeremy Winchester, Alexander Nemunaitis, Emily Nemunaitis, Ernest Bognar, Gladice Wallraven, Laura Stanbery, Adam Walter, Sep Sarshar & John Nemunaitis (2026) Preclinical assessment of GNE^{wt}/bi-shRNA-GNE^{M743T} lipoplex product development for GNE myopathy, Future Science OA, 12:1, 2635722, DOI: 10.1080/20565623.2026.2635722

To link to this article: https://doi.org/10.1080/20565623.2026.2635722

© 2026 The Author(s). Published by Informa UK Limited, trading as Taylor & Francis Group

View supplementary material

Published online: 02 Mar 2026.

Submit your article to this journal

Article views: 15

View related articles

View Crossmark data

Full Terms & Conditions of access and use can be found at
https://www.tandfonline.com/action/journalInformation?journalCode=ifso20

FUTURE SCIENCE OA
2026, VOL. 12, NO. 1, 2635722
https://doi.org/10.1080/20565623.2026.2635722

Taylor & Francis
Taylor & Francis Group

RESEARCH ARTICLE

OPEN ACCESS Check for updates

Preclinical assessment of GNE^{wt}/bi-shRNA-GNE^{M743T} lipoplex product development for GNE myopathy

Fabienne Kerneis[a], Christopher M Jay[a], Donald Rao[a], Jeremy Winchester[a], Alexander Nemunaitis[b], Emily Nemunaitis[b], Ernest Bognar[a], Gladice Wallraven[a], Laura Stanbery[a], Adam Walter[a,c], Sep Sarshar[d] and John Nemunaitis[a]

[a]Gradalis, Inc, Dallas, TX, USA; [b]Taylor Family Cancer Research Center, Maumee, OH, USA; [c]ProMedica, Toledo, OH, USA; [d]Solve GNE, Los Angeles, CA, USA

ABSTRACT

Aims: GNE myopathy is a heredity disease of unmet medical need associated with progressive skeletal muscle wasting, atrophy and weakness caused by mutations in the GNE gene. GNE plays a pivotal role in sialic acid production. Sialic acid is a critical part of glycoprotein, ganglioside and glycolipid cell-cell interaction which is necessary for normal skeletal muscle function. Previously we demonstrated safety and efficacy of the GNEwt gene lipoplex in one patient.

Methods: We engineered GNE^{M743T} and dual function GNEwt/bi-shRNA plasmids to evaluate GNE^{M743T} specific knockdown and GNEwt expression. Knockdown efficiency, protein expression, and functional rescue were assessed. A dose range study in mice quantified plasmid delivery and human GNE expression in muscle.

Results: We demonstrate effective plasmid function via knockdown of the GNE^{M743T} gene mutation and concurrent expression of GNEwt gene in a dose dependent manner. Similar in vitro increase in sialic acid production is shown between prior single function plasmid and GNE^{wt}/bi-shRNA-GNEM^{743T} dual function plasmid. Moreover, we demonstrate murine *in vivo* muscle delivery and expression of GNE^{wt} mRNA from the GNE^{wt}/bi-shRNA-GNE^{M743T} plasmid delivered via DOTAP-Cholesterol lipoplex following intravenous injection.

Conclusion: These results encourage future studies, potentially leading toward clinical testing of GNE^{wt}/bi-shRNA-GNE^{M743T} lipoplex for GNE myopathy.

ARTICLE HIGHLIGHTS

- GNE^{wt}/bi-shRNA-GNE^{M743T} dual function plasmid expresses GNE protein and knocks down GNE^{M743T}.
- Transfection with GNE^{wt}/bi-shRNA-GNE^{M743T} results in increased sialic acid expression *in vitro*.
- GNE^{wt}/bi-shRNA-GNE^{M743T} plasmid demonstrates delivery and expression in murine model.

ARTICLE HISTORY
Received 5 January 2026
Accepted 18 February 2026

KEYWORDS
Plasmid; bi-shRNA; GNE; myopathy; GNE M743T

1. Introduction

GNE (UDP-N-acetylglucosamine 2-epimerase/N-acetylmannosamine kinase) myopathy, formerly known as Inclusion Body Myopathy 2, Distal Myopathy with Rimmed Vacuoles, Nonaka Myopathy, Quadriceps Sparing Myopathy or Hereditary Inclusion Body Myopathy is an ultra-rare autosomal recessive non-inflammatory muscle disease characterized by early adult onset and progressive debilitating muscle dysfunction inherited through a variety of mutations of the GNE gene [1,2]. GNE^{M743T} is of higher incidence in people of Persian Jewish decent [2]. It is a well-accepted hypothesis that reestablishment of GNE^{wt} function via delivery of expressive GNE^{wt} gene will improve muscle sialic acid production and relieve muscle deterioration. Moreover, diminishing the adverse activity of GNE^{M743T} by knockdown with bi-shRNA-GNE^{M743T} we may further reduce muscle deterioration related to GNE^{M743T} protein associated myopathy and adverse competition with GNE^{wt} protein.

GNE^{wt} protein is the rate limiting enzyme that catalyzes the first two steps of the biosynthesis of sialic acid [3]. Sialic acids are negatively charged monosaccharides typically found as the terminal sugars on glycoconjugates. They play pivotal roles in cellular processes such as cell signaling, cell adhesion, cell migration and inflammation

CONTACT John Nemunaitis jnemunaitis@gradalisinc.com Gradalis, Inc, 2545 Golden Bear Dr., Suite 110, Carrollton, TX 75006, USA.
Supplemental data for this article can be accessed online at https://doi.org/10.1080/20565623.2026.2635722.
© 2026 The Author(s). Published by Informa UK Limited, trading as Taylor & Francis Group
This is an Open Access article distributed under the terms of the Creative Commons Attribution-NonCommercial License (http://creativecommons.org/licenses/by-nc/4.0/), which permits unrestricted non-commercial use, distribution, and reproduction in any medium, provided the original work is properly cited. The terms on which this article has been published allow the posting of the Accepted Manuscript in a repository by the author(s) or with their consent.

events [4]. GNE Myopathy-associated GNE mutations have been shown to reduce sialic acid production which is essential for proper folding, stabilization, and function of skeletal muscle glycoproteins [5–8]. GNE mutations resulting in hyposialyation of muscle glycoproteins appear to contribute to myofibrillar degeneration and loss of normal muscle function [9]. Thus, most in the field conclude that impaired GNE function [10,11], and/or reduced expression [12] is a key pathogenic factor in GNE myopathy. Indeed, Penner et al. [13] characterized several different GNE mutations and demonstrated altered activity of GNE enzyme related to mutation correlated with varying degrees of severity, as assessed by downstream enzyme kinetics of ManNAc phosphorylation using a radiolabeled phosphate assay. More recently, using a patient-derived induced pluripotent stem-cell model, Schmitt et al implicated defective myogenesis as an additional contributing factor for GNE myopathy [14]. GNE deficiency impaired myogenesis was demonstrated in human muscle cell line C2C12 with GNE knockout [15]. These observations further implicate GNE deficiency not only resulting in reduction of GNE enzyme activity but also impaired muscle myogenesis.

Lack of sialic acid however is not the only fundamental component to GNE myopathy, rather the underlying mechanism also involves deficiency in the ability to properly synthesize and regulate sialic acid due to GNE gene mutations encoding crucial enzymes for sialic acid production [16]. Mutated GNE gene function also disrupts ability to restore normal sialic acid production in muscle cells.

Therapeutic opportunities for patients with GNE myopathy are limited. Treatment options remain limited, with aceneuramic acid being the only approved therapy in Japan as of 2020. As a result, palliative management of disease symptomology is required [17–27]. We thus initiated a preclinical exploration of the GNE^{wt}/bi-shRNA-GNE^{M743T} lipoplex with the intent to improve the management of GNE myopathy.

The mutant GNE variant protein M743T has significantly reduced enzymatic activity when compared to GNE^{wt}. This effect was related to a single point mutation leading to a substitution of threonine from methionine at position 743 and relates to a change in oligomeric state, and possibly altered protein folding of GNE [3,28]. GNE is known to form multimeric structures. The monomeric form is inactive, while the dimeric and hexameric forms exhibit different enzymatic activities, with the hexameric form showing proficiency in both epimerase and kinase activities [29]. Bennmann et al. [30] found that the M743T variant had 4.5 times increase in O-GlcNAcylation compared to GNE^{wt}. Moreover, the half-life of the M743T variant was more than 2-fold the half-life of GNE^{wt} protein. These factors provide competitive advantage of GNE^{M743T} protein compared to GNE^{wt} protein and support the "push and pull" strategy to lower GNE^{M743T} activity while concurrently enhancing GNE^{wt} protein expression. Weidemann et al. [28] also demonstrated a reduced solubility and lower isoelectric point of the GNE^{M743T} protein in comparison to the GNE^{wt} protein and further demonstrated that the phosphorylation of the GNE^{M743T} protein influenced its isoelectric point. These observations likely relate to the results described by Bennmann. It has also been shown that O-GlcNAcylation extends the half-life of the GNE^{M743T} compared to GNE^{wt} protein activity thereby further contributing to the pathogenesis and severity of GNE myopathy. Removal of O-GlcNAc increases the GlcNAc 2-epimerase activity and the N-acetylmannosamine kinase activity of the M743T variant. O-GlcNAcylation plays a significant role in protein stability, enzyme activities and protein structure conformation. These alterations can also influence enzyme specificity [31–34]. Simultaneous replenishment of wildtype GNE and depletion of the competitive M743T mutant GNE, we hypothesize will more effectively restore functional GNE oligomer complex and muscle support function of GNE.

Previously we demonstrated evidence of improved transgene expression of GNE^{wt} mRNA and protein in correlation with subsequent increased production of sialic acid in CHO-Lec3 cells (with GNE deletion) *in vitro* along with *in vivo* models and clinical human evidence of benefit [35–38]. We also complexed the GNE expression plasmid with a cationic liposome, composed of 1,2-dioleoyl-3-trimethylammonium-propane (DOTAP) and cholesterol (GNE-Lipoplex) and demonstrated dose related safety in BALB/c mice with IV injection [9,39]. These results demonstrated correlation of the GNE^{wt} plasmid transfection with GNE transgene and protein expression at the desired target site, murine muscle, and provided sufficient evidence in murine model of safety at dose levels ≤40μg via IV delivery. We also demonstrated safety and improvement in local muscle strength correlating with enhancement of recombinant GNE (rGNE) muscle transgene expression and consequent increase of cell surface sialic acid following IM injection and later IV infusion of GNE-Lipoplex in a single patient with late stage GNE myopathy [37,38].

We now describe a novel upgraded GNE expression plasmid designed to achieve concurrent knockdown of GNE^{M743T} mutation and expression of GNE^{wt}, a dual function plasmid. The dual function plasmid has a bi-shRNAi

expression unit engineered on the same plasmid with the GNE^{wt} expression cassette. We also evaluated the final product lipoplex formulation (GNE^{wt}/bi-shRNA-GNE^{M743T} lipoplex) in a pilot murine study to determine dose range, delivery and expression of the drug to muscle tissue. We hypothesized that concurrent reduction in GNE^{M743T} protein will remove interference of disease related GNE^{M743T} competitive action and will optimize functionality of elevated GNE^{wt} protein expression [30].

2. Materials and methods

2.1. GNE clones and plasmid construction

Construction of the GNE clones and plasmid components describe in this assessment are compared to previous results as well as concurrent available murine models. A summary of performed experiments and planned studies including therapeutics, animal models, delivery and safety considerations are summarized in Supplemental Figure S1.

2.2. GNE^{M743T} target plasmid

A GNE^{M743T} target plasmid was created using pUMVC3 plasmid backbone (Aldevron, Fargo ND) by inserting the human GNE coding sequence, with the GNE^{M743T} variant behind CMV promoter.

2.3. GNE^{wt}/bi-shRNA-GNE^{M743T} dual function plasmids

Dual function plasmids express wild-type GNE and GNE^{M743T} knockdown bi-shRNA. Four (4) GNE^{wt}/bi-shRNA-GNE^{M743T} dual function plasmids were constructed to determine optimal functional knockdown of the GNE^{M743T} mutant transcripts and expression of GNE^{wt}. The pUMVC3 plasmid was the backbone for cloning. GNE^{wt} coding sequence was inserted together with bi-shRNA sequence in the plasmid. Two different bi-shRNA target sequences against the GNE^{M743T} variant were inserted at 2 possible locations, resulting in 4 different combinations of constructs (See Table 1 for bi-shRNA sequence and location). The GNE^{wt}/bi-shRNA-GNE^{M743T} constructs were co-transfected with the GNE^{M743T} target plasmid for GNE^{M743T} specific knockdown activity assessment by Restriction Fragment Length Polymorphism (RFLP) assay (described below). The GNE^{wt}/bi-shRNA-GNE^{M743T} plasmids and the GNE^{M743T} target plasmid were constructed by Epoch Life Science (Missouri City, TX).

2.4. GNE^{wt} plasmid

GNE^{wt} plasmid was described and tested in prior publication [35]. The GNE^{wt} plasmid is in the same pUMVC3 backbone as the GNE^{M743T} target and GNE^{wt}/bi-shRNA-GNE^{M743T} dual function plasmids.

2.5. Cell culture

HEK 293 (ATCC CRL-1573, Gaithersburg, MD) was maintained in a T225 culture flask with DMEM (ATCC, Manassas, VA) medium supplemented with 10% heat inactivated FBS and 2 mM L-Glutamine. After transfection, cells were cultured with 2% FBS.

Table 1. GNE^{wt}/bi-shRNA-GNE^{M743T} dual function plasmid design.

Construct	Target sequence	Placement of bi-shRNA unit
Construct #1	CCTGCTGGGTGCTGCCAGCAC<u>C</u>GG	Replace Intron-A (before the GNE^{wt} sequence)
Construct #2	CCTGCTGGGTGCTGCCAGCAC<u>C</u>GG	Behind the GNE^{wt} sequence
Construct #3	CTGCTGGGTGCTGCCAGCAC<u>C</u>GGT	Replace Intron-A (before the GNE^{wt} sequence)
Construct #4	CTGCTGGGTGCTGCCAGCAC<u>C</u>GGT	Behind the GNE^{wt} sequence

bi-shRNA target sequence against GNE^{M743T} mutation and the location of the bi-shRNA in relation to the GNE^{wt} coding sequence on the dual function plasmid. The underlined "<u>C</u>" is the single nucleotide mutation change from GNE^{wt} to GNE^{M743T}.

K562 KO (with GNE knocked out, was generously provided by Natalia Gomez-Ospina of Stanford University) and K562 wildtype (ATCC, Manassas, VA) were cultured in RPMI (ATCC, Manassas, VA) medium supplemented with 10% heat inactivated FBS and 2 mM L-Glutamine.

2.6. GNE^{wt}/bi-shRNA-GNE^{M743T} lipoplex

The Gradalis DOTAP:Chol Liposome formulation has been published [40]. Briefly, DOTAP and Cholesterol powders at 10:9 molar ratio are dissolved in ethanol and then injected into aqueous buffer (D5W) to create raw liposomes. The raw liposomes are buffer exchanged to remove the ethanol and volume adjusted to create the stock liposome with 10 mM DOTAP, 9.0 mM Cholesterol, in D5W buffer, with < 0.5% residual ethanol. The GNE^{wt}/bi-shRNA-GNE^{M743T} is diluted to 0.8 mg DNA/mL and then mixed with stock liposomes (1:1 mix ratio) to create the final GNE^{wt}/bi-shRNA-GNE^{M743T} lipoplex. The final product concentration is 5.0 mM DOTAP, 4.5 mM Cholesterol, 0.4 mg DNA/mL, in D5W buffer. QC testing of the GNE^{wt}/bi-shRNA-GNE^{M743T} lipoplex final product includes: safety (sterility, endotoxin, and mycoplasma), lipid identity (thin layer chromatography), DNA identity (restriction digest), DNA concentration (Abs260) purity, and physical properties (OD400, Particle Size, Zeta Potential).

2.7. Cell transfection by electroporation

HEK 293 cells were grown to 80–90% confluence, harvested using trypsin-EDTA, centrifuged, and then resuspended in OptiMEM at a concentration of 2e6 cells/mL. 0.8e6 cells in 0.4 mL were transferred to a 4 mm gap electroporation cuvette and mixed with plasmids at a varied concentration. Cells were electroporated at 200 V, 1000 µF with infinite resistance and exponential decay, using the BioRad Gene Pulser Xcell (BioRad, Hercules, CA). After electroporation, cells were transferred to 6 wells plates at a concentration of 0.4e6 cells per well with 2.0 mL of cell-appropriate media and cultured for 24h or 48h before harvest.

2.8. Cell transfection by DNA-lipoplex

K562 KO cells were harvested, centrifuged, and resuspended in OptiMEM media. GNE^{wt}/bi-shRNA-GNE^{M743T} lipoplex was mixed with cells at a varied concentration per 4e6 cells in 1 mL and incubated for 2 hours at 37 °C. After the incubation, GNE^{wt}/bi-shRNA-GNE^{M743T} lipoplex cell mixture was seeded in 6-well plates at 2e6 cells per well with 2 mL media and grown 48 hours.

2.9. Restriction fragment length polymorphism (RFLP) assay

Freshly harvested cells or frozen cells pellets were thawed on ice, and total RNA was extracted using Monarch® Total RNA Miniprep Kit (New England Biolabs, Ipswich, MA). The concentration of extracted RNA was measured with Nanodrop (Thermo Scientific, Waltham, MA). 1–3ug of total RNA was reverse transcribed using LunaScript® RT SuperMix Kit and random primers (New England Biolabs). cDNA synthesis was done in 20 µL or 40 µL reaction based on manufacturer instructions. cDNA was PCR amplified at the GNE^{M743T} region with designed primer set to create a BstXI restriction enzyme sequence for GNE^{wt}, but not for the GNE^{M743T} variant (Adaptor PCR sequence and BstXI digest is illustrated in Table 2). PCR reaction mixture (25 µL) consisted of Taq 2X Master Mix from NEB (NEB #M0270) with 3–5 µL of cDNA and 0.5 µL each of 1 µM PCR primers. PCR was performed with the Applied Biosystems SimpliAmp Thermal Cycler under standard PCR condition (briefly, 94 °C for 2 minutes, cycles at 94 °C for 15 seconds, 60 °C for 30 seconds and 72 °C for 1 minute for 25–30 cycles then incubated at 72 °C for 4 minutes and hold at 4 °C). RT-PCR amplified DNA was cut using BstXI enzyme (10 µL of PCR product were digested with 20 units of BstXI (NEB) for 45 minutes at 37 °C) and run on a 4% agarose gel (Invitrogen, Carlsbad CA).

The gel image was captured with ChemiDoc MP Imaging System (Bio-Rad). ImageJ software was used to quantify the band intensity for each PCR product and calculate the ratio between GNE^{wt} and GNE^{M743T} and determine percent knockdown. Briefly, the band of interest on the gel image were boxed and the intensity of boxed band was quantified. Quantified bands were used for the mutant to wild-type ratio. Each wild-type to

Table 2. RFLP primer design and BstXI recognition. The underlined bold and italicized 6 palindromic bases are the recognition sequence for restriction enzyme BstXI. The forward and reverse PCR primer set sequences are shown, PCR forward primer as shown below has a built in CCA to create the 5′ portion of the BstXI recognition sequence. The PCR products copied from GNE^{wt} cDNA have the BstXI recognition sequence, thus cut by BstXI. On the other hand, GNE^{M743T} with single nucleotide mutation does not contain the 3′ portion of BstXI recognition sequence, thus uncut. The amplicon is 214 bp, BstXI cut product is 186 bp; two products can be readily separated on a 4% agarose gel. Comparative PCR product intensity can be quantified by using image J program.

	Cut site ↓	
BstXI enzyme recognition	5′ cCA nNNNNNTGG 3′	Expected result
PCR forward primer	TGACCCCGCCCTGCTGGGTGCCACCAGCA	
PCR reverse primer	ATGTCCTTCCGAGTGAGAGA	
GNE^{WT}	TGACCCCGCCCTGCTGGGTGCCACCAGCATGGTTCTGG	Cut
GNE^{M743T}	TGACCCCGCCCTGCTGGGTGCCACCAGCACGGTTCTGG	No Cut

mutant ratio was compared within the same sample load thus truly represents the ratio between mutant and wild-type GNE in each sample analyzed.

2.9. Western blot

Cell pellets were lysed using M-PER reagent (ThermoFisher Scientific, Waltham, MA) per manufacturer instructions. Protein concentration was determined using the Bradford assay kit (ThermoFisher Scientific) with the Epoch plate reader at 595 nm (Agilent BioTek, Santa Clara, CA). Cell lysate samples (approximately 20 to 40 µg) were run on a Mini-Protean Tetra Vertical Electrophoresis Cell and 4–20% Mini-PROTEAN TGX Stain-free Precast Gel (BioRad) and 1X TRIS/Glycine/SDS buffer for 90 min at 75 V/3A/300W. Protein transfer was carried out using the Trans-Blot Turbo System (BioRad) and TransBlot Turbo Mini 0.2 µm PVDF Transfer Pack (BioRad). Samples were transferred at 1.3 A/25V for 10 minutes. Following transfer, the membrane was blocked using EveryBlot Blocking Buffer for 5 min at room temperature. The membrane was incubated with anti-GNE polyclonal antibody (rabbit) (VWR, Radnor, PA) at 1:10,000 dilution and α/β-Tubulin antibody #2148 (rabbit) (Cell Signaling Technology, Danvers, MA) at 1:1,000 dilution. Secondary antibody was goat anti-rabbit IgG (H + L) HRP at a dilution of 1:10,000 (VWR). The membrane was washed and then ECL Western Blotting substrate (BioRad) was added for visualization using the ChemiDoc MP system (BioRad). Quantification of Western the blot bands was done using the ChemiDoc Image lab software, according to the BioRad instructions. The software calculated the intensity for each band, and the GNE to Tubulin ratio was calculated and normalized to the control group.

2.10. Sialic acid assay/statistics

Transfected K562 KO cell pellets were lysed using the freeze/thaw method with dry ice bath and dry heat block at 37 °C followed by mechanical shearing to lyse the cells. Lysates were analyzed using the Sialic Acid Assay Kit (Millipore Sigma, St. Louis, MO) as directed. Sialic acid samples were read at 549 nm in the Epoch plate reader. The concentration of the unknown samples was calculated against the kit standard curve and then sialic acid concentration normalized against protein concentration performed using the Bradford Kit Assay (ThermoFisher Scientific) [40]. Replicate samples were tested (n = 4) with the average and standard deviation calculated per treatment group. An ANOVA was conducted to determine whether the means of the three groups differed significantly. Upon identifying a statistically significant result from the ANOVA, pairwise t-tests were subsequently performed to assess specific differences between individual groups.

2.11. Murine study

A dose range mouse study was designed to evaluate GNE^{wt}/bi-shRNA-GNE^{M743T} lipoplex maximum tolerated dose, drug delivery to the muscle, and GNE expression. The animal study was performed at Charles River (Durham, NC). Female BALB/c mice (n = 3 per group, approximately 20 g each) were treated with 25ug, 50 µg, or 100ug DNA-Lipoplex. Mice were injected through the tail vein with a slow IV push of 6–8 seconds. Animals were sacrificed at 24 hr, tissue was preserved in RNALater and shipped to Frontage Labs (Deerfield Beach, FL) for assay.

2.12. Preparation of DNA and RNA from murine study tissues for tissue delivery and expression analysis

Frontage Labs extracted total gDNA from mouse tissues using the Chemagic DNA 400 Kit on the Chemagic 360 machine (Perkin Elmer, Waltham, MA). Total RNA was extracted using Tri Reagent (Molecular Research Center, Cincinnati, OH) by manual method. Both gDNA and total RNA was quantified by Abs260. DNA quality was assessed by 0.8% gel electrophoresis and RNA quality was assessed via Bioanalyzer (Agilent Technologies, Santa Clara, CA).

2.13. End-point PCR

An aliquot of extracted gDNA was returned to Gradalis for end-point PCR. Custom designed pGNE^{wt}/bi-shRNA-GNE^{M743T} plasmid specific primers (forward: GAAGGCCCAGAGCATCCTAA and reverse: CGTTGTGTAGTCCAGAACCAT) were used with 2.5 ng template gDNA for end-point PCR (33 cycles using the SimpliAmp Thermal Cycler from Applied Biosystems). End-point PCR reactions were loaded on 4% agarose E-gel (Invitrogen) and the gel image was captured with ChemiDoc MP Imaging System (Bio-Rad).

2.14. ddPCR for murine tissue DNA delivery analysis/statistics

The remaining gDNA was analyzed at Frontage Labs by ddPCR analysis. A custom designed primer/probe set was tested and demonstrated to specifically detect the GNE plasmid DNA, without cross-reacting with endogenous mouse GNE. gDNA samples were restriction digested with HindIII and BsrGI-HF to linearize the template DNA. ddPCR was performed using 10 ng restriction digested gDNA per reaction. The assay lower limit of quantitation (LLOQ) was 20 copies. Results were reported as copies GNE DNA per 10 ng total gDNA input. ddPCR results are reported as average of each treatment group (n = 3), with standard deviation, and t-test analysis against the control group for significant differences.

2.15. RT-ddPCR for murine tissue RNA expression analysis/statistics

Total RNA was extracted from tissue, DNase digested to remove residual DNA, and converted to cDNA. The commercially available TaqMan Human GNE (hGNE) kit (HS01103400_m1, Thermo Fisher) was used to detect GNE cDNA. The cDNA ddPCR assay was tested and demonstrated to specifically detect the plasmid expressed human GNE RNA, without cross-reacting with endogenous mouse GNE. The RT-ddPCR assay LLOQwas 10 copies. Results were reported as copies hGNE cDNA per 10 ng total RNA input. RT-ddPCR results are reported as average of each treatment group (n = 3), with standard deviation, and t-test analysis against the control group for significant differences.

3. Results

3.1. Construction of GNE^{wt}/bi-shRNA-GNE^{M743T} dual function plasmids and GNE^{wt}, GNE^{M743T} expression plasmids

There is currently no GNE^{M743T} expressing cell line available. In order to assess the effectiveness of GNE^{M743T} specific knockdown, a GNE^{M743T} target expression plasmid (Supplemental Figure S2A) was constructed for co-transfection with GNE^{wt}/bi-shRNA-GNE^{M743T} dual function plasmids.

Four different GNE^{wt}/bi-shRNA-GNE^{M743T} dual function plasmids were designed to express GNE^{wt} and concurrently knockdown GNE^{M743T} expression. The GNE^{wt}/bi-shRNA-GNE^{M743T} plasmids were constructed with an expression cassette of GNE^{wt} cDNA and a bifunctional shRNA unit in tandem. (Supplemental Figure S2B,C) The expression cassette was inserted behind the CMV promoter. The bifunctional shRNA unit is either in front of GNE coding sequence (Supplemental Figure S2B) or behind (Supplemental Figure S2C). Four GNE^{wt}/bi-shRNA-GNE^{M743T} plasmids were designed to compare efficiency of GNE^{M743T} knockdown and GNE^{wt} expression. Two sets of bi-shRNA target sequences have slightly different seed region sequences shown in Table 1 (construct #1 and #2 vs. #3 and #4). The seed region sequence affects the efficiency of RNAi process, by locating the single nucleotide mutation sequence at slightly different locations of the seed sequence, the efficiency and selectivity could be different as we have observed with prior product construction to other molecular targets [40–43].

The location of bi-shRNA-GNE^{M743T} relative to the CMV promoter directed transcription unit could also affect the efficiency of shRNA process and GNE^{wt} expression. The bi-shRNA sequences either replaced the Intron A sequence in front of the GNE cDNA (construct #1 and 3) or placed behind GNE cDNA (construct #2 and #4). CMV Intron A contains a series of secondary structures that resemble the secondary structures of bi-shRNA. Placing the bi-shRNA at Intron A may improve the secondary structure processing which may affect activity. Each of the four bi-shRNA plasmid constructs were made with a RNAi target sequence match at the GNE^{M743T} location to differentiate GNE^{wt} from GNE^{M743T}. The RNAi target sequences and their locations are summarized in Table 1.

3.2. Dose related expression of GNE and knockdown of GNE^{M743T} assayed by restriction fragment length polymorphism (RFLP)

There is currently no antibody available to differentiate GNE^{wt} from GNE^{M743T} protein. We utilized the RFLP method to differentiate GNE^{wt} vs. GNE^{M743T} at the mRNA level. An adaptor PCR forward primer was designed to incorporate BstXI recognition sequence for PCR (See Table 2). The amplified PCR products for GNE^{wt} contain the restriction enzyme BstXI recognition sequence while PCR products for GNE^{M743T} do not. Consequently, GNE^{wt} PCR products are digested by BstXI resulting in a smaller size (28 bp shorter) fragment than GNE^{M743T} PCR product and can be visualized by gel electrophoresis.

Untransfected HEK293 cells express low levels of endogenous GNE^{wt} mRNA (See Figure 1A Lane 1). HEK293 cells were transfected with equal amounts of GNE^{wt} expression plasmid and GNE^{M743T} target plasmid and show similar levels of GNE^{wt} and GNE^{M743T} mRNA expression (Figure 1A Lanes 2–3).

Comparison of the four GNE^{wt}/bi-shRNA-GNE^{M743T} dual function plasmids co-transfected with GNE^{M743T} target plasmid is shown in Figure 1A, Lanes 4–7. Conceptually, Co-transfection of dual function plasmid and GNE^{M743T}

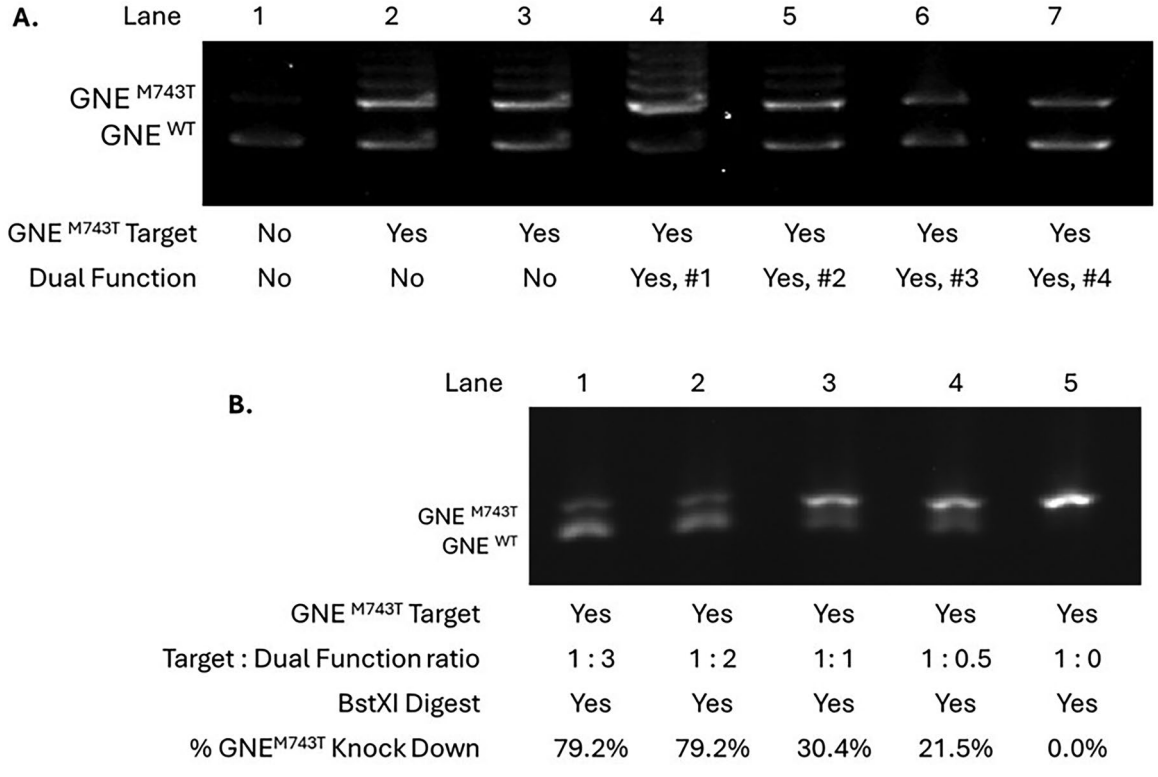

Figure 1. GNE^{wt}/bi-shRNA-GNE^{M743T} Dual Function Plasmids Demonstrate Dose Related Knockdown of GNE^{M743T} Expression Target. A) Four GNE^{wt}/bi-shRNA-GNE^{M743T} constructs and GNE^{M743T} expression target plasmid were tested for expression compared to HEK293 cells. RNA from transfected cells were harvested 24 hours post transfection and processed for RFLP. HEK293 cells no transfection (Lane 1). Co-transfection with equal amount of GNE^{wt} and GNE^{M743T} expression target plasmid (Lane 2 and 3). Co-transfection with equal amount of GNE^{M743T} expression target plasmid and each of four GNE^{wt}/bi-shRNA-GNE^{M743T} dual function constructs (Lanes 4–7). B) Co-transfection of GNE^{M743T} target expression plasmid with a decreasing dose of GNE^{wt}/bi-shRNA-GNE^{M743T} dual function construct #3 (lanes 1–5). Lane 5 transfection with target plasmid only. Transfected cells were harvested 48 hours post transfection.

target plasmid is anticipated to express GNE^{wt} and reduce GNE^{M743T} expression. Construct #1 showed ineffective GNE^{M743T} knockdown and noticeable reduced of GNE^{wt} mRNA expression (Figure 1A, Lane 2 and 3). Construct #2 showed more GNE^{M743T} mRNA than GNE^{wt} mRNA. Construct #3 and #4 both show reduced GNE^{M743T} expression and GNE^{wt} expression. Construct #3 demonstrated effective GNE^{M743T} knockdown but modest GNE^{wt} expression. Construct #4 showed GNE^{M743T} knockdown compared to control but lesser impact on GNE^{M743T} knockdown than construct #3 (Based on raw value comparison from the gel band scan quantitation, Figure 1A).

The initial screen described above (Figure 1A) was with equal amount of GNE^{wt}/bi-shRNA-GNE^{M743T} dual function plasmid and GNE^{M743T} target plasmid. We next explored dose response of the GNE^{wt}/bi-shRNA-GNE^{M743T} plasmid in terms of GNE^{M743T} knockdown and GNE^{wt} expression. We selected construct #3 based on results in Figure 1A to explore the dose response relationship in GNE^{M743T} knockdown and GNE^{wt} expression (Figure 1B). HEK293 cells were co-transfected with varied amounts of construct #3 (from 0x to 3x relative to GNE^{M743T} target plasmid) together with a fixed amount (5 µg) GNE^{M743T} expressing target plasmid. 24 hours post transfection, total cellular RNA were isolated and RT-PCR with BstXI adaptor primer set, PCR products were digested with BstXI and run on a 4% agarose gel. Increasing doses of construct #3 resulted in dose dependent decrease of GNE^{M743T} transcripts in comparison to GNE^{M743T} target plasmid only transfection (Figure 1B, Lanes 4-1 vs. Lane 5) indicate knockdown by GNE^{M743T} targeting bi-shRNA component of dual function plasmid; concurrent to decrease in GNE^{M743T} transcript, GNE^{wt} transcripts were increased (GNE^{wt} transcribed from GNE^{wt}/bi-shRNA-GNE^{M743T} dual function plasmid) (Figure 1B lane 5, no GNE^{wt}/bi-shRNA-GNE^{M743T} plasmid to lane 1 high GNE^{wt}/bi-shRNA-GNE^{M743T} dose concentration). The mutant bands of each combination transfection (Figure 1B lanes 1–4) were compared to mutant expression plasmid only transfection (Figure 1B lane 5) to estimate knockdown efficiency using ImageJ software. The optimal knockdown was demonstrated at 1:2 and 1:3 ratio of GNE^{M743T} target expression plasmid to dual function plasmid (79.2% knockdown Figure 1B lanes 1, 2). Within the analysis timeframe, knockdown was saturated at 1:2 ratio and dose dependent, therefore 1:2 was chosen as the optimal dose ratio for further analysis. GNE^{wt} expression showed steady increase as increasing dose of GNE^{wt}/bi-shRNA-GNE^{M743T} were applied at transfection. It appears the GNE^{wt} transcript expression from the GNE^{wt}/bi-shRNA-GNE^{M743T} plasmid was not adversely affected by the knockdown of GNE^{M743T} transcripts, GNE^{wt} mRNA expression from the dual function plasmid alone was not assessed in this study. Construct #4 showed similar dose response (Data not shown).

3.3. GNE^{wt}/bi-shRNA-GNE^{M743T} dual function plasmid expresses GNE protein

We next tested the GNE^{wt}/bi-shRNA-GNE^{M743T} dual function plasmid expression of GNE wt protein without interference from the GNE^{M743T} knockdown component. GNE knockout K562 cells (K562 KO) present a platform to analyze the expression of GNE protein from the vector without endogenous GNE background. Human GNE protein has a known molecular weight range from 66 to 79 kDa, β-Tubulin with molecular size range around 50–55 kDa close to GNE size was selected as the endogenous expressed protein load control. K562 KO cells were transfected with either GNE^{wt} or GNE^{wt}/bi-shRNA-GNE^{M743T} construct #3 Lipoplex. Both GNE^{wt} and GNE^{wt}/bi-shRNA-GNE^{M743T} treated cells showed expression of GNE protein by western blot analysis (Figure 2, Lanes 2 and 3) while liposome only treatment did not result in appearance of GNE protein (Figure 2, Lane 1). The GNE band and β-Tubulin band intensities were quantified, quantified value of GNE from each treatment group was normalized with β-Tubulin load control of the empty liposome control for comparison. Quantitatively, the GNE^{wt}/bi-shRNA-GNE^{M743T} construct #3 expressed a similar amount of GNE protein as the GNE^{wt} plasmid (Figure 2) demonstrating comparable GNE expression without significant interference from the bi-shRNA unit. The same secondary antibody was used for both GNE and β-Tubulin which may affect the precise quantification of relative GNE protein level but should not be widely different.

3.4. GNE expression resulting in increased sialylated protein in transfected cells

Total cellular sialic acid as the result of GNE^{wt}/bi-shRNA-GNE^{M743T} construct #3 transfection was assessed. K562 KO cells were transfected with DNA-Lipoplex and then cultured 2 days in 2.5% serum media after transfection. Reduced serum is necessary to limit sialic acid contribution from serum. Cells were harvested, cell pellets were lysed, total cellular sialic acid was quantified and normalized against protein concentration (n = 4 per treatment group). K562 KO cells treated with GNE^{wt} lipoplex or GNE^{wt}/bi-shRNA-GNE^{M743T} lipoplex show increased total sialic acid vs. empty lipoplex control indicating increase in sialylation by both plasmids (Figure 3). The ANOVA approach showed that

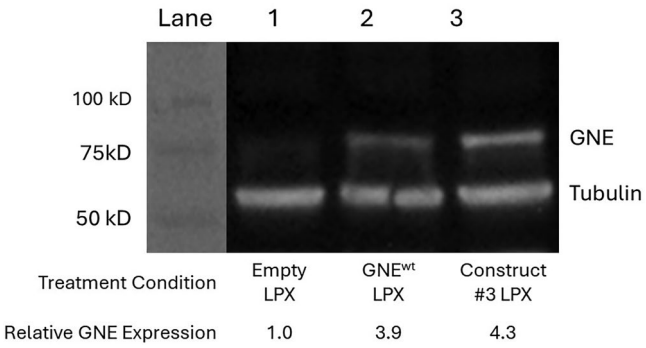

Figure 2. Expression of GNE Protein from Transfected K562 KO Cells. K562 cells with GNE knockout (K562 KO) transfected with GNE^{wt}/bi-shRNA-GNE^{M743T} lipoplex and analyzed by Western Blot for GNE protein expression. Top band is GNE. Bottom band is β-Tubulin (protein load control). Lane 1: Empty liposome, Lane 2: GNE^{wt} lipoplex, Lane 3: Dual function construct #3 GNE^{wt}/bi-shRNA-GNE^{M743T} lipoplex. Western Blot band intensities were quantified using the ChemiDoc software. The relative GNE expression was calculated by GNE band intensity normalized to load control β-tubulin band intensity. The same secondary antibody was used for both GNE and β-Tubulin. This may influence the determination of relative GNE expression. LPX: lipoplex.

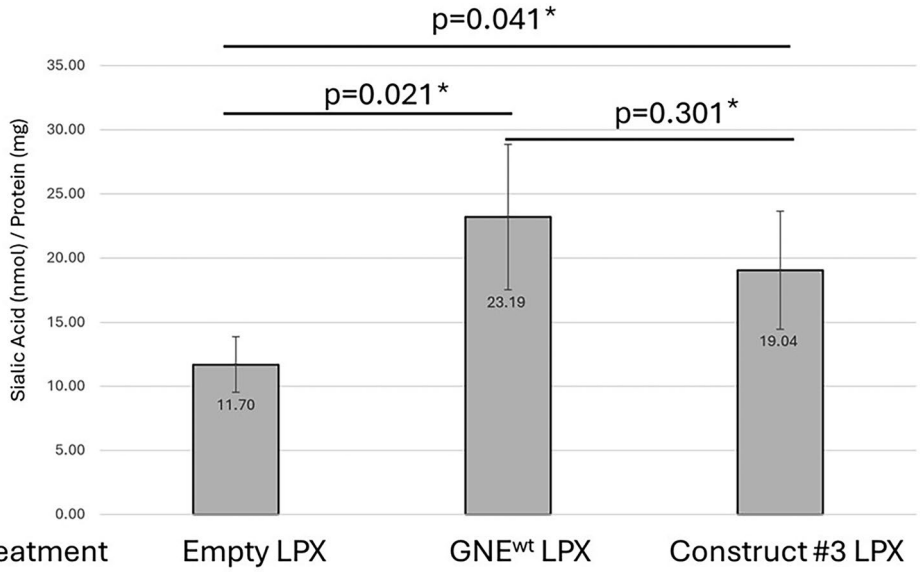

Figure 3. Total Cellular Sialic Acids Increase After Expression Plasmid Transfection. K562 KO cells transfected with various lipoplexes. Both GNE^{wt} and GNE^{wt}/bi-shRNA-GNE^{M743T} construct #3 demonstrates increased total cellular sialic acid over control, demonstrating GNE plasmid functionality. Each treatment condition represents an average of 4 replicates, with standard deviation error bars. P-value from the ANOVA analysis is 0.015. [* t-test]. LPX: lipoplex.

there is a statistically significant difference among the group means (p-value = 0.015). Further evaluation by t-test shows significant increase in sialic acid in treatment groups relative to control (p=0.021 and p=0.041 respectively). There was no significant difference in total cellular sialic acid levels comparing GNE^{wt} vs. GNE^{wt}/bi-shRNA-GNE^{M743T} transfected cells. This result further demonstrates functional activities of transfected plasmids in improving cellular sialylation, and that the bi-shRNA component has no negative effect on GNE^{wt} activity.

3.5. Detection of GNE^{wt}/bi-shRNA-GNE^{M743T} plasmid in muscle of in vivo systemic delivered GNE^{wt}/bi-shRNA-GNE^{M743T} lipoplex

The next step was to evaluate a dose range of GNE^{wt}/bi-shRNA-GNE^{M743T} lipoplex *in vivo* and determine if the plasmid lipoplex formulation was delivered to the quadriceps muscle using a murine model. Muscle is known to be difficult organ for systemic delivery of gene therapy agents [44]. A pilot study was designed to determine if formulated lipoplex was delivered to muscle. While GNE is characterizing by a sparing of the quadriceps muscle, the quadriceps was chosen to because it provides sufficient mass for downstream studies. A follow up study is

planned to evaluate other muscle tissues. Normal BALB/c mice were chosen because the study scope was to determine maximum tolerated dose and drug delivery to the muscle, not drug efficacy. The animals (n = 3 per group) were treated with a single IV injection of GNE^{wt}/bi-shRNA-GNE^{M743T} lipoplex at 25 µg, 50 µg, or 100 µg and then sacrificed 24 hours after treatment. Animals receiving 50ug dose showed lethargy and ruffled fur which was identified as the maximum tolerated dose. One animal in the 100 µg group was found dead the day after treatment, therefore 100 µg was identified as intolerable dose. Quadriceps tissues were harvested for nucleic acid extraction and PCR analysis. Mouse quadriceps from the 50 µg GNE^{wt}/bi-shRNA-GNE^{M743T} lipoplex treatment group (n = 3) were extracted for total DNA and analyzed for drug delivery, as a first look before additional samples were tested. An end-point PCR assay with custom designed primers was designed to detect plasmid GNE without cross-reacting with the mouse gDNA. The plasmid DNA was detected in all (n = 3) 50 µg dose treated quadriceps samples, but not in the 0 µg untreated mice (Figure 4). Results indicate successful delivery of plasmid DNA into mouse quadriceps muscle at maximum tolerated dose.

3.6. Quantification of GNE^{wt}/bi-shRNA-GNE^{M743T} plasmid DNA and human GNE^{wt} mRNA from muscle of in vivo treated mice further demonstrates delivery and expression with lipoplex formulation

Based on the initial end-point PCR results for the 50ug muscle samples, the delivery and expression of GNE^{wt}/bi-shRNA-GNE^{M743T} lipoplex in each dose group was quantified using ddPCR analysis of quadriceps tissue.

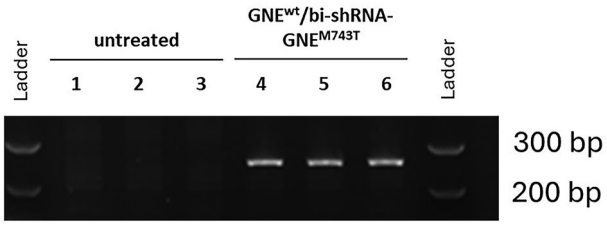

Figure 4. Detection of GNE^{wt}/bi-shRNA-GNE^{M743T} Dual Function Plasmids in Murine Muscle After Treatment. Normal laboratory strain mice were treated with GNE^{wt}/bi-shRNA-GNE^{M743T} dual function lipoplex. Three mice per group were treated with 50 µg of GNE^{wt}/bi-shRNA-GNE^{M743T} lipoplex via single tail vein injection and tissues collected 24 hours after treatment. PCR primers were specifically designed to amplify GNE^{wt}/bi-shRNA-GNE^{M743T}. Total DNA harvested from quadriceps muscles of treated mice (lanes 4–6) demonstrated the presence of plasmid DNA compared to non-treated mice (lanes 1–3).

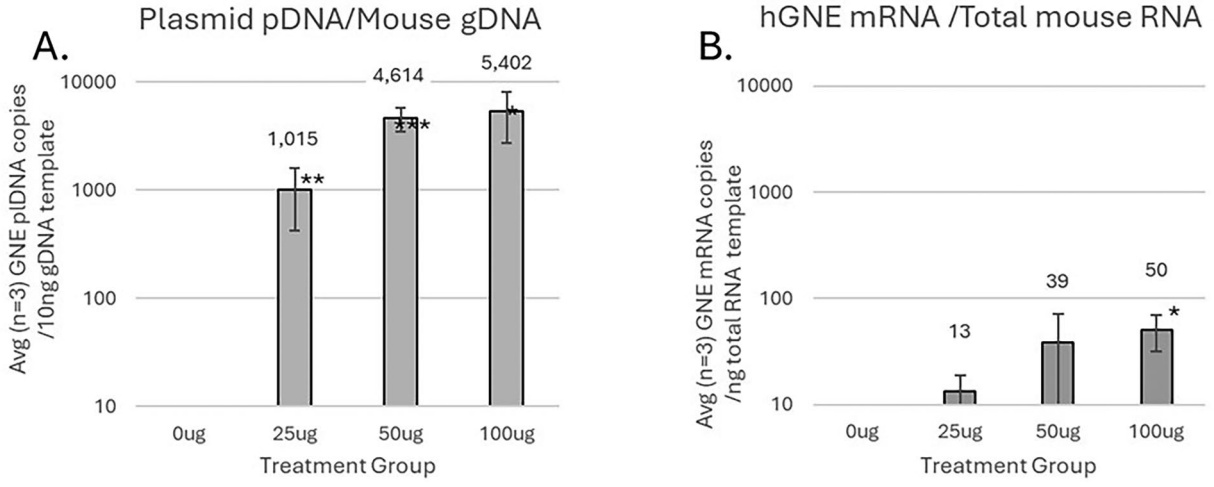

Figure 5. ddPCR Results Demonstrate GNE^{wt}/bi-shRNA-GNE^{M743T} Lipoplex Delivery and Expression After Single IV Injection of Test Article. 0 µg group is no treatment control. 25 µg, 50 µg, and 100 µg are GNE^{wt}/bi-shRNA-GNE^{M743T} lipoplex treatment groups. Data presented is the average for each treatment group (n = 3), with standard deviation error bars and t-test to evaluate for significant differences relative to the control group (*$p < 0.05$, **$p < 0.01$, ***$p < 0.001$). A) Mouse quad muscle tissue had a dose-related delivery of increasing amount of GNE plasmid DNA injected (delivery) compared to control (0 µg). B) RT-ddPCR results demonstrate GNE^{wt}/bi-shRNA-GNE^{M743T} expression of human GNE^{wt} mRNA in treated mouse quad muscle. Muscle tissue had a dose-related expression of human GNE mRNA transcribed from dual function plasmid (expression). pDNA: plasmid DNA, hGNE: human GNE.

Custom DNA ddPCR primers were designed to detect human GNE portion of plasmids without cross reacting with the mouse genomic DNA. The ddPCR results demonstrate delivery of GNE^{wt}/bi-shRNA-GNE^{M743T} plasmid to the quadriceps in the GNE^{wt}/bi-shRNA-GNE^{M743T} lipoplex treated groups (Figure 5A). There was no human GNE expression plasmid detected in the 0 µg group. PCR results demonstrate a dose-response delivery of plasmid DNA to the muscle tissue following a single IV injection.

Mouse muscle tissue was extracted for total RNA, converted to cDNA, and then assayed for human GNE mRNA expression using a commercially available human GNE (hGNE) primer/probe set. The assay was verified to detect human GNE cDNA, without cross-reacting with mouse GNE cDNA. The cDNA from mouse quadriceps tissue was analyzed by ddPCR assay (Figure 5B). Human GNE cDNA was not detected in the 0 µg group. Human GNE cDNA was detected in each GNE^{wt}/bi-shRNA-GNE^{M743T} lipoplex treatment group. The results demonstrate that the single IV injection of DNA-lipoplex was delivered, and human GNE mRNA was expressed in mouse muscle quadriceps in a dose-dependent fashion.

4. Discussion

Previously, in preclinical testing and with management of one patient with advanced GNE myopathy, we showed that plasmid delivery of GNE^{wt} plasmid via DOTAP-cholesterol lipoplex is feasible (DNA delivery/RNA expression) to quadriceps muscle via IV infusion [38]. Treatment was reasonably well tolerated as measured beyond 1 year of IV dosing every 2 months. Furthermore, we demonstrated evidence of clinical benefit related to stabilization of muscle strength/function in association with systemic GNE^{wt} lipoplex infusion [38]. However, in the majority of muscles tested over time, strength/function was only minimally or not improved at all. We postulated given the reported relationship of GNE^{M743T} mutant protein inhibitory effect to GNE^{wt} activity that a dual function GNE^{wt}/bi-shRNA-GNE^{M743T} lipoplex product concurrently reduce the inhibitory mutant and replenish wt may be necessary to enhance GNE^{wt} gene replacement activity. In this report, we demonstrated the designed dual function plasmid with successful activity of both components. Specifically concurrent knockdown of GNE^{M743T} and expression of GNE^{wt} protein and mRNA as well as related sialic acid production. We also verified in a murine model the successful delivery of GNE^{wt}/bi-shRNA-GNE^{M743T} plasmid and expression of human GNE mRNA in muscle tissue. Based on these results as rationale for therapeutic opportunity for GNE myopathy patients with M743T mutation, we showed feasibility of concurrent GNE^{wt} expression with knockdown of GNE^{M743T}. Using this "push and pull" strategy to express GNE^{wt} in combination with concurrent GNE^{M743T} knockdown we believe we have shown proof of principle for additional testing, including further preclinical development of this strategy toward clinical testing of patients with GNE^{M743T} myopathy.

The bi-shRNA based technology is an exquisitely specific knockdown technology, with capacity to target single nucleotide RNA alteration. We have previously published design and activity of several novel bi-shRNA lipoplexes, including constructs designed to knockdown *KRAS, PDX1, STMN1, EWS/FLI1* and *FURIN* that have demonstrated specificity, safety and efficacy in oncogene knockdown in preclinical and clinical testing [40–43,45,46]. Preclinically, we have demonstrated target specificity and effective knockdown of *KRAS* G12 mutations and pancreatic and duodenal homeobox-1 (*PDX1*) using bi-shRNA constructs specific to each target. Knockdown was demonstrated in mutant specific cell lines and murine xenograft models [42]. Additionally, with bi-shRNA EWS/FLI LPX we demonstrated safety and survival benefit in a murine xenograft model of Ewing's sarcoma. Gemogenovatucel-T (Vigil) is the most advanced bi-shRNAi technology. It is a triple function immunotherapy that is prepared using autologous tumor cells transfected with a dual function plasmid, which expresses *GM-CSF* and a bi-shRNA component to knockdown mRNA expression of *FURIN [47]*. Vigil has been studied in multiple clinical trials and has demonstrated remarkable safety and significant evidence of efficacy recently highlighted by RMAT designation in a unique subpopulation of advanced ovarian cancer patients [48–50]. Furthermore, Phase 1 clinical trial with bi-shRNA-STMN1 demonstrated proof of principle to mechanism of bi-shRNA inhibitory action by identifying the predicted target specific cleavage product via next generation sequence assessment testing [46].

For each bi-shRNA design, we routinely examine the potential off-target effects of bi-shRNA constructs via mRNA-Seq profiling. mRNA-Seq profiles from various doses of the bi-shRNA constructs transfected cells are compared against un-transfected or mock transfected cells. The bioinformatics analysis of mRNA-Seq profiles comparisons is focused on differentially expressed genes (DEG), particular emphasis on mRNAs with reduced

expression. mRNA-Seq identified genes with reduced expression as the result of bi-shRNA transfection are further analyzed for homology with bi-shRNA target sequence. If numerous highly homologous gene sequences are identified through this process, alternative constructs are designed.

Several FDA approved products involving plasmid delivery have been proven to justify FDA recommendation for use in clinical management [38,51]. Plasmid construction can also be engineered to provide prolonged gene expression without integration in the genome or risk of replication [52,53]. Persistence elements (i.e., inverted terminal repeats [54,55]) can be incorporated into plasmid design to transiently prolong gene expression *in vitro* and *in vivo* thereby minimizing time of treatment timepoints and frequency of patient treatments. Inducible promoters can also be considered to promote expression in the presence of a positive regulator or in the absence of a negative regulator [56]. Taking promoter-enhancer sequence elements from a tissue specific gene to include in our expression plasmid, may for example, lead to as much as a 70-fold increased gene expression *in vivo* [57]. Such an approach will need to be explored as a possible future plasmid design if short-term GNE expression and GNE^{M743T} knockdown demonstrate evidence of clinical muscle function enhancement. To evaluate the efficacy of the dual function "push–pull" approach, suitable *in vitro* and *in vivo* models of GNE myopathy are required, particularly for the M743T mutation. The mechanism and specificity of bi-shRNA requires an exact sequence match to the target sequence. While no ideal human M743T model currently exists, GNE knockout or mutant cell lines, including HEK293 and K562 systems, have been used to study GNE biology, with HEK293 cells providing a practical platform for transfection and monitoring sialylation changes under serum-depleted conditions [58–61]. Genetically edited muscle cell models also reveal altered F-actin and reduced epimerase activity [62]. However, patient-derived M743T muscle cells show inconsistent sialylation changes [63]. *In vivo*, *Gne* knock-in and transgenic mouse models demonstrate variable phenotypes, including renal failure, hyposialylation, and muscle involvement [63–68]. These models are based on the murine GNE sequence that is significantly divergent from human sequence around the M743T region and therefore would not be suitable for testing the human specific bi-shRNA sequence. Dual function constructs with murine GNE mRNA sequence and bi-shRNA tailored to the specific murine GNE sequence is necessary to validate for mutation-specific knockdown and rescue activity *in vivo* with Gne^{M743T} knock in mouse model, they could be utilized to test dual function capacity.

However, GNE^{M743T} is only one of more than 376 genetic variations involving GNE myopathy syndrome [12,69]. RNAi targeted therapy is limited in that it only impacts the specific mutation, in this case GNE^{M743T}, not all variants, and clinical evidence of efficacy in patients with GNE^{M743T} myopathy will act as proof of principle for individualized plasmid constructs targeting other mutations.

Other therapeutic assessments involving non plasmid based products have thus far shown limited evidence of benefit to patients with GNE myopathy. Oral administration of n-acetylmannosamine (ManNAc) in advanced GNE myopathy patients was well tolerated and induced sustained increases in circulating levels of free n-acetlyneuraminic acid (Neu5Ac) [19]. Subsequently, a Phase 2 trial was conducted on 12 patients with GNE myopathy to further characterize ManNAc replacement therapy. Patients demonstrated a slower rate of decline and small transient improvement in extremity strength as well as muscle function enhancement via evaluation by "Adult Myopathy Assessment Tool" (AMAT [17]). However, these changes did not translate into statistically significant or durable functional benefit over longer follow up. Additionally, the biochemical assessment of treated patient samples did show intracellular biosynthesis of increased Neu5Ac following ManNAc [18,19] which support the conclusion that ManNac does not demonstrate significant durable functional muscle benefit.

Sialic acid (Neu5Ac/g) supplementation along with intravenous immunoglobulin (IVIG) treatment also showed limited efficacy and demonstrated transient muscle strength improvement with no effect on muscle sialylation [20]. Transient adverse events including nausea, vomiting, headache, anorexia, and constipation were observed, thereby limiting further treatment.

Testing of an extended release formulation of aceneuramic acid (Ace-ER) initially demonstrated positive activity in Japanese variant GNE myopathy patients. A comparative single and multiple ascending dose Phase 1 trial of immediate release aceneuramic acid (Ace-IR) and Ace-ER showed that patients receiving Ace-ER had fewer adverse events [21]. Patients receiving Ace-ER achieved significantly higher serum levels of aceneuramic acid, compared to no increase for the Ace-IR group. A follow up study in Japan further evaluated Ace-ER vs. placebo in GNE myopathy patients showed statistically significant preservation of muscle strength [22,23].

However, a Phase 3 global trial of Ace-ER failed to demonstrate stabilization or improvement in muscle function extremity scores, knee extensor strength or improved GNE myopathy-Function Activity scale over placebo [24].

6'-Sialyllactose (6SL) is present in high concentrations in human milk and can be converted into sialic acid via an alternative pathway involving sialidases (also known as neuraminidases). Earlier preclinical studies showed that oral administration of 6SL in a GNE myopathy mouse model resulted in the recovery of muscle function and volume even during the symptomatic phase of the disease [70]. Based on these observations, two clinical trials were carried out to analyze the effects of oral doses of 6SL in patients with GNE myopathy. The first trial included 10 patients in a pharmacokinetic study and 20 patients in an efficacy and safety study over 96 weeks [25]. This trial lacked a placebo arm after the first 12 weeks but observed sustained improvement or stabilization in proximal muscle strength. The second trial followed 11 patients over 48 weeks (6 in the 6SL arm/5 in the placebo arm) [26]. This study did not demonstrate superior muscle strength compared to the placebo group, however biological activation through significant re-sialylation of cells showed a trend toward slowed muscle fat degeneration on MRI.

Several different GNE mutations beyond GNE^{M743T} have demonstrated altered activity of GNE enzyme function as assessed by downstream enzyme kinetics [13]. All mutations reduce GNE^{wt} enzymatic activity which may relate to gradual muscle function deterioration over many years rather than sudden myopathy. In support of this, Savelkoul et al. [11] suggested that GNE myopathy defects related to sialylation appear gradually in muscle tissue in relation to disruptions in GNE enzyme function.

It has also been reported that despite decreased biochemical activity of mutated GNE, the overall sialic acid levels in patients can be unaffected [71] or unrelated to clinical significance. Some mouse models carrying the GNE M743T alleles generated through homologous recombination in fact do not develop myopathy, which limits full evaluation of products designed to impact GNE myopathy [64,72]. Although the transgenic mouse model *Gne*(-/-)hGNED176V-Tg, which expresses the human GNE p.D176V variant shows functional myopathy, this is not the M743T variant [65].

Prevalence of GNE myopathy is suggested by Celeste et al. and is predicted to involve ~40,000 patients worldwide. A recent publication attempting to determine the disease prevalence allele frequencies from population genetic databases estimated the prevalence to be 11–88 individuals per million [69]. However, only about 800 patients with clinical symptomatology have been reported, the reason for the discrepancy is unclear [12]. It could be due to under-diagnosis particularly outside USA, Japan and Europe and may be related to null mutation in GNE likely being associated with embryonic lethality.

In conclusion, evidence presented here supports further testing and preclinical evaluation of the dual function GNE^{wt}/bi-shRNA-GNE^{M743T} lipoplex as a potential future therapy for patients with GNE myopathy with the GNE^{M743T} mutation. Further work will involve IND discussion with FDA and possible additional evaluation in HEK cells with the GNE^{M743T} human mutation, use of patient cells harboring GNE^{M743T} mutation and/or GNE^{M743T} knock in mice model including plasmid uptake by other organs and toxicity evaluation as well as.

Acknowledgments

The authors would like to thank Brenda Marr for her competent and knowledgeable assistance in the preparation of the manuscript. We thank Natalia Gomez-Ospina of Stanford University for kindly providing the K562-GNE knockout cells. This research has not been previously presented.

Ethical statement

No approval was required for this study.

Authors' contributions

FK, CMJ, JW, DR were responsible for data curation, formal analysis, investigation and writing – original draft and writing – review and editing. EB provided supervision, data curation and writing – review and editing of the manuscript. AN and EN contributed to writing – original draft and writing – review and editing. LS provided supervision, writing – original draft and writing – review and editing. AW and SS and GW were responsible for formal analysis and writing – review and editing of the manuscript. GN provided writing – review and editing. JN provided supervision, conceptualization and manuscript – review and editing.

Disclosure statement

FK, CMJ, DR, EB, GW, LS and AW are employed by Gradalis, Inc and own stock. JN is a board member, employee and owns stock in Gradalis, Inc. AN, GN, and EN have no conflict of interest to disclose. SS is a pro bono scientific advisor to Solve GNE.

Funding

Funding for this project was provided by Solve GNE. The funders had no role in study design, data collection and analysis, decision to publish, or preparation of the manuscript.

Data availability statement

The data that support the findings of this study are available from the corresponding author upon reasonable request.

References

Papers of special note have been highlighted as either of interest (•) or of considerable interest (••) to readers.

[1] Huizing M, Krasnewich DM. Hereditary inclusion body myopathy: a decade of progress. Biochim Biophys Acta. 2009; 1792(9):881–887. doi: 10.1016/j.bbadis.2009.07.001
[2] Kaback M, Lopatequi J, Portuges AR, et al. Genetic screening in the Persian Jewish community: a pilot study. Genet Med. 2010;12(10):628–633. doi: 10.1097/GIM.0b013e3181edef5b
[3] Stasche R, Hinderlich S, Weise C, et al. A bifunctional enzyme catalyzes the first two steps in N-acetylneuraminic acid biosynthesis of rat liver. Molecular cloning and functional expression of UDP-N-acetyl-glucosamine 2-epimerase/ N-acetylmannosamine kinase. J Biol Chem. 1997;272(39):24319–24324.
[4] Varki A. Sialic acids as ligands in recognition phenomena. Faseb J. 1997;11(4):248–255. doi: 10.1096/fasebj.11.4.9068613
[5] Huizing M, Rakocevic G, Sparks SE, et al. Hypoglycosylation of alpha-dystroglycan in patients with hereditary IBM due to GNE mutations. Mol Genet Metab. 2004;81(3):196–202. doi: 10.1016/j.ymgme.2003.11.012
[6] Keppler OT, Hinderlich S, Langner J, et al. UDP-GlcNAc 2-epimerase: a regulator of cell surface sialylation. Science (1979). 1999;284(5418):1372–1376. doi: 10.1126/science.284.5418.1372
[7] Ricci E, Broccolini A, Gidaro T, et al. NCAM is hyposialylated in hereditary inclusion body myopathy due to GNE mutations. Neurology. 2006;66(5):755–758. doi: 10.1212/01.wnl.0000200956.76449.3f
[8] Langer GA. The structure and function of the myocardial cell surface. Am J Physiol. 1978;235(5):H461–8. doi: 10.1152/ajpheart.1978.235.5.H461
[9] Jay CM, Levonyak N, Nemunaitis G, et al. Hereditary inclusion body myopathy (HIBM2). Gene Regul Syst Bio. 2009; 3:181–190. doi: 10.4137/grsb.s2594
[10] Krause S, Aleo A, Hinderlich S, et al. GNE protein expression and subcellular distribution are unaltered in HIBM. Neurology. 2007;69(7):655–659. doi: 10.1212/01.wnl.0000267426.97138.fd
[11] Savelkoul PJ, Manoli I, Sparks SE, et al. Normal sialylation of serum N-linked and O-GalNAc-linked glycans in hereditary inclusion-body myopathy. Mol Genet Metab. 2006;88(4):389–390. doi: 10.1016/j.ymgme.2006.04.011
[12] Celeste FV, Vilboux T, Ciccone C, et al. Mutation update for GNE gene variants associated with GNE myopathy. Hum Mutat. 2014;35(8):915–926. doi: 10.1002/humu.22583
[13] Penner J, Mantey LR, Elgavish S, et al. Influence of UDP-GlcNAc 2-epimerase/ManNAc kinase mutant proteins on hereditary inclusion body myopathy. Biochemistry. 2006;45(9):2968–2977. doi: 10.1021/bi0522504
[14] Schmitt RE, Smith D, Cho DS, et al. Myogenesis defects in a patient-derived iPSC model of hereditary GNE myopathy. NPJ Regen Med. 2022;7(1):48. doi: 10.1038/s41536-022-00238-3
[15] Neu CT, Weilepp L, Bork K, et al. GNE deficiency impairs myogenesis in C2C12 cells and cannot be rescued by ManNAc supplementation. Glycobiology. 2024;34(3). doi: 10.1093/glycob/cwae004
[16] Mullen J, Alrasheed K, Mozaffar T. GNE myopathy: history, etiology, and treatment trials. Front Neurol. 2022;13:1002310. doi: 10.3389/fneur.2022.1002310
[17] Harris-Love MO, Joe G, Davenport TE, et al. Reliability of the adult myopathy assessment tool in individuals with myositis. Arthritis Care Res (Hoboken). 2015;67(4):563–570. doi: 10.1002/acr.22473
[18] Carrillo N, Malicdan MC, Leoyklang P, et al. Safety and efficacy of N-acetylmannosamine (ManNAc) in patients with GNE myopathy: an open-label phase 2 study. Genet Med. 2021;23(11):2067–2075. doi: 10.1038/s41436-021-01259-x
[19] Xu X, Wang AQ, Latham LL, et al. Safety, pharmacokinetics and sialic acid production after oral administration of N-acetylmannosamine (ManNAc) to subjects with GNE myopathy. Mol Genet Metab. 2017;122(1–2):126–134. doi: 10.1016/j.ymgme.2017.04.010
[20] Sparks S, Rakocevic G, Joe G, et al. Intravenous immune globulin in hereditary inclusion body myopathy: a pilot study. BMC Neurol. 2007;7(1):3. doi: 10.1186/1471-2377-7-3
[21] Suzuki N, Kato M, Warita H, et al. Phase I clinical trial results of aceneuramic acid for GNE myopathy in Japan. Trans Med Commun. 2018;3(1):7.

[22] Suzuki N, Mori-Yoshimura M, Katsuno M, et al. Phase II/III study of aceneuramic acid administration for GNE myopathy in Japan. J Neuromuscul Dis. 2023;10(4):555–566. doi: 10.3233/JND-230029
[23] Suzuki N, Mori-Yoshimura M, Katsuno M, et al. Safety and efficacy of aceneuramic acid in GNE myopathy: open-label extension study. J Neurol Neurosurg Psychiatry. 2024;95(11):1093–1094. doi: 10.1136/jnnp-2024-333853
[24] Lochmüller H, Behin A, Caraco Y, et al. A phase 3 randomized study evaluating sialic acid extended-release for GNE myopathy. Neurology. 2019;92(18):e2109–e2117. doi: 10.1212/WNL.0000000000006932
[25] Park YE, Park E, Choi J, et al. Pharmacokinetics and clinical efficacy of 6′-sialyllactose in patients with GNE myopathy: randomized pilot trial. Biomed Pharmacother. 2023;168:115689. doi: 10.1016/j.biopha.2023.115689
[26] Park YE, Choi J, Kim L, et al. A pilot trial for efficacy confirmation of 6′-sialyllactose supplementation in GNE myopathy: randomized, placebo-controlled trial. Mol Genet Metab. 2025;144(1):108614. doi: 10.1016/j.ymgme.2024.108614
[27] Pereira BL, Barbosa M, Granjo P, et al. Beyond sialylation: exploring the multifaceted role of GNE in GNE myopathy. Mol Genet Metab. 2025;144(4):109075. doi: 10.1016/j.ymgme.2025.109075
[28] Weidemann W, Reinhardt A, Thate A, et al. Biochemical characterization of the M712T-mutation of the UDP-N-acetylglucosamine 2-epimerase/N-acetyl-mannosaminekinase in hereditary inclusion body myopathy. Neuromuscul Disord. 2011;21(12):824–831. doi: 10.1016/j.nmd.2011.06.004
[29] Chen SC, Huang CH, Lai SJ, et al. Mechanism and inhibition of human UDP-GlcNAc 2-epimerase, the key enzyme in sialic acid biosynthesis. Sci Rep. 2016;6(1):23274. doi: 10.1038/srep23274
[30] Bennmann D, Weidemann W, Thate A, et al. Aberrant O-GlcNAcylation disrupts GNE enzyme activity in GNE myopathy. Febs J. 2016;283(12):2285–2294. doi: 10.1111/febs.13729
[31] Miranda FF, Thórólfsson M, Teigen K, et al. Structural and stability effects of phosphorylation: localized structural changes in phenylalanine hydroxylase. Protein Sci. 2004;13(5):1219–1226. doi: 10.1110/ps.03595904
[32] Chu CS, Lo PW, Yeh YH, et al. O-GlcNAcylation regulates EZH2 protein stability and function. Proc Natl Acad Sci USA. 2014;111(4):1355–1360. doi: 10.1073/pnas.1323226111
[33] Olivier-Van Stichelen S, Dehennaut V, Buzy A, et al. O-GlcNAcylation stabilizes beta-catenin through direct competition with phosphorylation at threonine 41. Faseb J. 2014;28(8):3325–3338. doi: 10.1096/fj.13-243535
[34] Charoensuksai P, Kuhn P, Wang L, et al. O-GlcNAcylation of co-activator-associated arginine methyltransferase 1 regulates its protein substrate specificity. Biochem J. 2015;466(3):587–599. doi: 10.1042/BJ20141072
[35] Jay C, Nemunaitis G, Nemunaitis J, et al. Preclinical assessment of wt GNE gene plasmid for management of hereditary inclusion body myopathy 2 (HIBM2). Gene Regul Syst Bio. 2008;2:243–252. doi: 10.4137/grsb.s728**Outlines the work by our group with the prior plasmid.
[36] Duan D. Considerations on preclinical neuromuscular disease gene therapy studies. In: Duan D, Mendell JR, editors. Muscle gene therapy. Cham: Springer International Publishing; 2019. p. 291–326.
[37] Nemunaitis G, Jay CM, Maples PB, et al. Hereditary inclusion body myopathy: single patient response to intravenous dosing of GNE gene lipoplex. Hum Gene Ther. 2011;22(11):1331–1341. doi: 10.1089/hum.2010.192**Clinical work with the prior plasmid.
[38] Nemunaitis G, Maples PB, Jay C, et al. Hereditary inclusion body myopathy: single patient response to GNE gene Lipoplex therapy. J Gene Med. 2010;12(5):403–412. doi: 10.1002/jgm.1450**Clinical work with the prior plasmid.
[39] Phadke AP, Jay C, Chen SJ, et al. Safety and in vivo expression of a GNE-transgene: a novel treatment approach for hereditary inclusion body myopathy-2. Gene Regul Syst Bio. 2009;3:89–101. doi: 10.4137/grsb.s2210
[40] Rao DD, Jay C, Wang Z, et al. Preclinical justification of pbi-shRNA EWS/FLI1 lipoplex (LPX) treatment for Ewing's sarcoma. Mol Ther. 2016;24(8):1412–1422. doi: 10.1038/mt.2016.93
[41] Rao DD, Luo X, Wang Z, et al. KRAS mutant allele-specific expression knockdown in pancreatic cancer model with systemically delivered bi-shRNA KRAS lipoplex. PLoS One. 2018;13(5):e0193644. doi: 10.1371/journal.pone.0193644
[42] Liu SH, Rao DD, Nemunaitis J, et al. PDX-1 is a therapeutic target for pancreatic cancer, insulinoma and islet neoplasia using a novel RNA interference platform. PLoS One. 2012;7(8):e40452. doi: 10.1371/journal.pone.0040452
[43] Rao DD, Maples PB, Senzer N, et al. Enhanced target gene knockdown by a bifunctional shRNA: a novel approach of RNA interference. Cancer Gene Ther. 2010;17(11):780–791. doi: 10.1038/cgt.2010.35
[44] Braun S. Non-viral vector for muscle-mediated gene therapy. In: Duan D, Mendell JR, editors. Muscle gene therapy. Cham: Springer International Publishing; 2019. p. 157–178.
[45] Anderson P, Ghisoli M, Crompton BD, et al. Pilot study of recurrent Ewing's sarcoma management with vigil/temozolomide/irinotecan and assessment of circulating tumor (ct) DNA. Clin Cancer Res. 2023;29(9):1689–1697. doi: 10.1158/1078-0432.CCR-22-2292
[46] Barve M, Wang Z, Kumar P, et al. Phase 1 trial of bi-shRNA STMN1 BIV in refractory cancer. Mol Ther. 2015;23(6):1123–1130. doi: 10.1038/mt.2015.14
[47] Senzer N, Barve M, Kuhn J, et al. Phase I trial of "bi-shRNAi(furin)/GMCSF DNA/autologous tumor cell" vaccine (FANG) in advanced cancer. Mol Ther. 2012;20(3):679–686. doi: 10.1038/mt.2011.269
[48] Walter A, Rocconi RP, Monk BJ, et al. Gemogenovatucel-T (Vigil) maintenance immunotherapy: 3-year survival benefit in homologous recombination proficient (HRP) ovarian cancer. Gynecol Oncol. 2021;163(3):459–464. doi: 10.1016/j.ygyno.2021.10.004
[49] Rocconi RP, Grosen EA, Ghamande SA, et al. Gemogenovatucel-T (Vigil) immunotherapy as maintenance in frontline stage III/IV ovarian cancer (VITAL): a randomised, double-blind, placebo-controlled, phase 2b trial. Lancet Oncol. 2020;21(12):1661–1672. doi: 10.1016/S1470-2045(20)30533-7

[50] Rocconi RP, Monk BJ, Walter A, et al. Gemogenovatucel-T (Vigil) immunotherapy demonstrates clinical benefit in homologous recombination proficient (HRP) ovarian cancer. Gynecol Oncol. 2021;161(3):676–680. doi: 10.1016/j.ygyno.2021.03.009
[51] Curreri A, Sankholkar D, Mitragotri S, et al. RNA therapeutics in the clinic. Bioeng Transl Med. 2023;8(1):e10374. doi: 10.1002/btm2.10374
[52] Ledwith BJ, Manam S, Troilo PJ, et al. Plasmid DNA vaccines: investigation of integration into host cellular DNA following intramuscular injection in mice. Intervirology. 2000;43(4–6):258–272. doi: 10.1159/000053993
[53] Chen Z, Yao J, Zhang P, et al. Minimized antibiotic-free plasmid vector for gene therapy utilizing a new toxin-antitoxin system. Metab Eng. 2023;79:86–96. doi: 10.1016/j.ymben.2023.07.003
[54] Aksentijevich I, Pastan I, Lunardi-Iskandar Y, et al. In vitro and in vivo liposome-mediated gene transfer leads to human MDR1 expression in mouse bone marrow progenitor cells. Hum Gene Ther. 1996;7(9):1111–1122. doi: 10.1089/hum.1996.7.9-1111
[55] Baudard M, Flotte TR, Aran JM, et al. Expression of the human multidrug resistance and glucocerebrosidase cDNAs from adeno-associated vectors: efficient promoter activity of AAV sequences and in vivo delivery via liposomes. Hum Gene Ther. 1996;7(11):1309–1322. doi: 10.1089/hum.1996.7.11-1309
[56] Vilaboa N, Voellmy R. Deliberate regulation of therapeutic transgenes. In: Templeton NS, editor. Gene and cell therapy: therapeutic mechanisms and strategies. Boca Raton, FL: Taylor & Francis/CRC Press; 2008. p. 619–636.
[57] Lu H, Zhang Y, Roberts DD, et al. Enhanced gene expression in breast cancer cells in vitro and tumors in vivo. Mol Ther. 2002;6(6):783–792. doi: 10.1006/mthe.2002.0813
[58] Singh R, Arya R. GNE myopathy and cell apoptosis: a comparative mutation analysis. Mol Neurobiol. 2016;53(5):3088–3101. doi: 10.1007/s12035-015-9191-5
[59] Chaudhary P, Sharma S, Singh R, et al. Elucidation of ER stress and UPR pathway in sialic acid-deficient cells: pathological relevance to GNEM. J Cell Biochem. 2021;122(12):1886–1902. doi: 10.1002/jcb.30148
[60] Devi SS, Yadav R, Mashangva F, et al. Generation and characterization of a skeletal muscle cell-based model carrying one single gne allele: implications in actin dynamics. Mol Neurobiol. 2021;58(12):6316–6334. doi: 10.1007/s12035-021-02549-w
[61] Yadav R, Devi SS, Oswalia J, et al. Role of HSP70 chaperone in protein aggregate phenomenon of GNE mutant cells: therapeutic lead for GNE myopathy. Int J Biochem Cell Biol. 2022;149:106258. doi: 10.1016/j.biocel.2022.106258
[62] Devi SS, Yadav R, Arya R. Altered actin dynamics in cell migration of GNE mutant cells. Front Cell Dev Biol. 2021;9:603742. doi: 10.3389/fcell.2021.603742
[63] Sela I, Yakovlev L, Becker Cohen M, et al. Variable phenotypes of knockin mice carrying the M712T Gne mutation. Neuromolecular Med. 2013;15(1):180–191. doi: 10.1007/s12017-012-8209-7
[64] Galeano B, Klootwijk R, Manoli I, et al. Mutation in the key enzyme of sialic acid biosynthesis causes severe glomerular proteinuria and is rescued by N-acetylmannosamine. J Clin Invest. 2007;117(6):1585–1594. doi: 10.1172/JCI30954
[65] Malicdan MC, Noguchi S, Nonaka I, et al. A Gne knockout mouse expressing human GNE D176V mutation develops features similar to distal myopathy with rimmed vacuoles or hereditary inclusion body myopathy. Hum Mol Genet. 2007;16(22):2669–2682. doi: 10.1093/hmg/ddm220
[66] Benyamini H, Kling Y, Yakovlev L, et al. Upregulation of hallmark muscle genes protects GneM743T/M743T mutated knock-in mice from kidney and muscle phenotype. J Neuromuscul Dis. 2020;7(2):119–136. doi: 10.3233/JND-190461
[67] Crowe KE, Zygmunt DA, Heller K, et al. Visualizing muscle sialic acid expression in the GNED207VTgGne-/- Cmah-/- model of GNE myopathy: a comparison of dietary and gene therapy approaches. J Neuromuscul Dis. 2022;9(1):53–71. doi: 10.3233/JND-200575
[68] Mitrani-Rosenbaum S, Yakovlev L, Becker Cohen M, et al. Pre-clinical assessment of AAVrh74.MCK.GNE viral vector therapeutic potential: robust activity despite lack of consistent animal model for GNE myopathy. J Neuromuscul Dis. 2022;9(1):179–192. doi: 10.3233/JND-210755
[69] Derksen A, Thompson R, Shaikh M, et al. Estimating the prevalence of GNE myopathy using population genetic databases. Hum Mutat. 2024;2024(1):7377504. doi: 10.1155/2024/7377504
[70] Yonekawa T, Malicdan MC, Cho A, et al. Sialyllactose ameliorates myopathic phenotypes in symptomatic GNE myopathy model mice. Brain. 2014;137(Pt 10):2670–2679. doi: 10.1093/brain/awu210
[71] Salama I, Hinderlich S, Shlomai Z, et al. No overall hyposialylation in hereditary inclusion body myopathy myoblasts carrying the homozygous M712T GNE mutation. Biochem Biophys Res Commun. 2005;328(1):221–226. doi: 10.1016/j.bbrc.2004.12.157
[72] Ito M, Sugihara K, Asaka T, et al. Glycoprotein hyposialylation gives rise to a nephrotic-like syndrome that is prevented by sialic acid administration in GNE V572L point-mutant mice. PLoS One. 2012;7(1):e29873. doi: 10.1371/journal.pone.0029873